Informatics in Medicine Unlocked 38 (2023) 101235

Contents lists available at ScienceDirect

Informatics in Medicine Unlocked

journal homepage: www.elsevier.com/locate/imu

Mathematical modelling and analysis of COVID-19 and tuberculosis transmission dynamics

Ram Singh [a,*], Attiq ul Rehman [a], Tanveer Ahmed [b], Khalil Ahmad [b], Shubham Mahajan [c,d], Amit Kant Pandit [e], Laith Abualigah [f,g,h,i,j,k], Amir H. Gandomi [l,m,*]

[a] Department of Mathematical Sciences, BGSB University, Rajouri, 185234, India
[b] Department of Mathematics, Al-Falah University, Faridabad, India
[c] Ajeenkya D Y Patil University, Pune, Maharashtra, 412105, India
[d] University Center for Research & Development (UCRD), Chandigarh University, Mohali, India
[e] School of Electronic and Communication, Shri Mata Vaishno Devi University, Katra, 182320, India
[f] Computer Science Department, Prince Hussein Bin Abdullah Faculty for Information Technology, Al al-Bayt University, Mafraq 25113, Jordan
[g] College of Engineering, Yuan Ze University, Taiwan
[h] Hourani Center for Applied Scientific Research, Al-Ahliyya Amman University, Amman 19328, Jordan
[i] Faculty of Information Technology, Middle East University, Amman 11831, Jordan
[j] Applied science research center, Applied science private university, Amman 11931, Jordan
[k] School of Computer Sciences, Universiti Sains Malaysia, Pulau Pinang 11800, Malaysia
[l] Faculty of Engineering and Information Technology, University of Technology Sydney, Ultimo, NSW, 2007, Australia
[m] University Research and Innovation Center (EKIK), Óbuda University, 1034 Budapest, Hungary

ARTICLE INFO

Keywords:
Modelling
COVID-19
Bifurcation
Optimal solution
Sensitivity analysis

ABSTRACT

In this paper, a mathematical model for assessing the impact of COVID-19 on tuberculosis disease is proposed and analysed. There are pieces of evidence that patients with Tuberculosis (TB) have more chances of developing the SARS-CoV-2 infection. The mathematical model is qualitatively and quantitatively analysed by using the theory of stability analysis. The dynamic system shows endemic equilibrium point which is stable when $\mathcal{R}_0 < 1$ and unstable when $\mathcal{R}_0 > 1$. The global stability of the endemic point is analysed by constructing the Lyapunov function. The dynamic stability also exhibits bifurcation behaviour. The optimal control theory is used to find an optimal solution to the problem in the mathematical model. The sensitivity analysis is performed to clarify the effective parameters which affect the reproduction number the most. Numerical simulation is carried out to assess the effect of various biological parameters in the dynamic of both tuberculosis and COVID-19 classes. Our simulation results show that the COVID-19 and TB infections can be mitigated by controlling the transmission rate γ.

1. Introduction

Recently, COVID-19 is posing a big threat to mankind around the world. Almost the entire world has been reeling under the repeated waves of COVID-19. The very first case of COVID-19 was reported in Wuhan city of China, in late 2019. This deadly virus was silently spreading to many countries till March 2020. Since 5 April 2020, every country has been suffering because of this virus. The COVID-19 patient asymptotically carried this virus and spread it to other susceptible individuals. Asymptotically and exposed persons are the main carriers of this virus. Till date there have been approximately 23,97,216 established cases and 1,62,956 deaths due to this epidemic disease [1–3]. Most cases of SARS-CoV-2 infection are self-limiting and have minimum symptoms. But it is well confirmed that the patients with elder age underlying endemic diseases such as hypertension, diabetes, tuberculosis (TB), and coronary heart disease are continuously raised risk of difficulties and mortality due to severe COVID-19 [4,5].

Like COVID-19, Tuberculosis (TB) is a life-threatening bacterial disease predominantly affecting the lungs. Tuberculosis is caused by mycobacterium bacteria that transmit through the air after coughing and sneezing. After launching many vaccination programes, this disease remains a problem worldwide. TB is a type of disease that increases

* Corresponding authors.
E-mail addresses: drramsinghmaths@gmail.com (R. Singh), attiqrehman24@gmail.com (A.U. Rehman), tanveerahmed@bgsbu.ac.in (T. Ahmed), kahmad49@gmail.com (K. Ahmad), mahajanshubham2232579@gmail.com (S. Mahajan), amitkantpandit@gmail.com (A.K. Pandit), Aligah.2020@gmail.com (L. Abualigah), gandomi@uts.edu.au (A.H. Gandomi).

https://doi.org/10.1016/j.imu.2023.101235
Received 22 January 2023; Received in revised form 28 March 2023; Accepted 28 March 2023
Available online 31 March 2023

due to environmental factors such as open drainage of sewage in residential areas, discharge of household wastes in a residential area, open water storage tanks, etc. In 2017, almost ten million new tuberculosis populations were estimated and appeared globally [6]. However, approximately three million cases have been registered in India, and it is the top in the universe [7]. But, tuberculosis-related deaths went down from 0.00056 year^{-1} in 2000 to 0.00032 year^{-1}, although they still caused approximately one and a half million death cases in India in 2016. Moreover, the prevalence of latent mycobacterium tuberculosis infection is also at a very high stage in India [8].

Both COVID-19 and tuberculosis spread in human body through a common path via upper respiratory tract [9–13]. There are shreds of evidence that patients with tuberculosis and latent mycobacterium tuberculosis infection have a high risk of SARS-CoV-2 infection, and afterwards, their immune system gets weakened and they receive COVID-19 infection very early [14–19]. The relationship between COVID-19 and tuberculosis is particularly common in the public health system in India. Therefore, India is one of the top contributors due to endemic tuberculosis, with the highest cases in the world [6,20]. Also, isolation of contacts and cases for the control of COVID-19 gives problems in low socioeconomic tuberculosis households [21].

Considering these circumstances, the large burden of active TB cases in India along with community transmission, localized estimation of the infection, a hot-spot of COVID-19 and birth due to the COVID-19 epidemic among tuberculosis patients in India is warranted. This would enable the allocation of resources towards implementing and developing effective public health interventions in such defected populations. With this area of study, we try to estimate the number of tuberculosis people infected due to SARS-CoV-2 and vital illnesses during the COVID-19 epidemic in Delhi, India. Markov's chance system was applied to assume the amount of severe and mild/moderate illness [22].

Two frameworks are used to approximate the amount of infectious COVID-19 cases, (a) Taking public health strategies/interventions (b) Taking public health strategies like social distancing and isolation of contacts and cases. The total contributed to the case pool was approximately 31% for workplace contact, 50% for household contact, 21% for social contact. The estimated mitigation gains by the social distancing, intervention lockdown, case and contact isolation 96% for workplace contacts, was 25% for household contacts and 70% for social contacts [23,24].

We also considered that the impact of social distancing and lockdown interventions might be shown after seven days which is half of the maximum incubation period. The basic reproduction number $\mathcal{R}_0$ under person health interventions was measured by multiplying the fractions of COVID-19 infected patients. The total number of confirmed cases of TB infection in 2018 for the world was obtained from the WHO report 2019, which are approximately 2.64 million cases [6,13]. The total number of COVID-19 and TB co-infected patients with acute illness was considered as 54% as per a study conducted in China [21]. The various mathematical models on endemic disease are analysed by the authors [25,26].

Both infectious diseases Tuberculosis and COVID-19 mostly effect on lungs of a human. On this aforementioned consequence, we make a mathematical co-infection epidemic model which is useful to our society.

Our study aims to formulate SE_HE_CIR compartmental model to evaluate the total number of COVID-19 infected patients with the help of the progression rate from exposed COVID-19 class to infectious class to control this epidemic. This proposed compartmental model assumes a closed population that might not be considered in earlier models [12]. But, due to the lockdown, people's movements are effectively controlled in the world. This study needs to control with precautions to assess the risk of vital illness COVID-19 in tuberculosis patients. This data is captured from China, a highly affected country in the world. The prevalence of tuberculosis in general individuals might not be the same as the prevalence of tuberculosis in COVID-19 between TB cases; the study is already applied the above assumption.

This paper develops a deterministic compartmental mathematical model to incorporate the COVID-19 and tuberculosis co-infection. We extend the work of author [27] in which the authors presented the mathematical model for tuberculosis transmission in the zoonotic areas with the existence of positive equilibrium. But in our work, we incorporate the effects of COVID-19 on TB cases. This co-infection is reported in India in which TB and COVID-19 affected the people simultaneously [11].

The paper is arranged as follows. Section 2 is devoted to the mathematical model formulation. The basic preliminaries of the proposed model are given in Section 3. The mathematical analysis of the model is done in Section 4. In Section 5, the optimal model is analysed. In Section 6, the bifurcation analysis is derived. Sensitivity analysis is carried out in Section 7. The numerical simulation is performed in Section 8. The conclusion is drawn in Section 9.

2. Formulation of mathematical model

In order to formulate the SE_HE_CIR mathematical model for transmission dynamics of TB and COVID-19 virus in a homogeneous population. We divide the entire population into five classes, namely susceptible class $S(t)$, exposed Tuberculosis class $E_H(t)$, exposed COVID-19 class $E_C(t)$, infected class $I(t)$ and recovered class $R(t)$, respectively. Therefore, the total host population is constant and we have

$$N = S + E_H + E_C + I + R.$$

Thus, the mathematical model in the form of a set of differential equations is given below.

$$\begin{aligned}
\frac{dS}{dt} &= \Omega - \left(\frac{\alpha I}{N} + \mu\right)S + f\phi E_H,\\
\frac{dE_H}{dt} &= \frac{\alpha I}{N}q(1-p)S - (\mu+\tau)E_H - \phi E_H,\\
\frac{dE_C}{dt} &= \frac{\alpha I}{N}(1-q)(1-p)S - (\mu+\gamma)E_C,\\
\frac{dI}{dt} &= \tau E_H + \gamma E_C + \frac{\alpha I}{N}pS - (\mu+d+r)I + (1-f)\phi E_H,\\
\frac{dR}{dt} &= rI - \mu R.
\end{aligned} \tag{1}$$

The new population entering in susceptible class is at the constant rate Ω. Let μ be the rate at which the population is dying naturally. The susceptible population are getting exposed to TB infection at the rate q. A fraction $(1-q)$ of population is exposed COVID-19 infection. Also, p is fraction of people who are in contact with infected population and become infected and got active TB disease. It is also assumed that the TB population is vaccinated against COVID-19 at the constant rate f. ϕ is assumed to be the death rate due to COVID-19 and α is the infection contact rate, respectively. After vaccination some people are recovered at the rate r and d is the TB-induced death rate. The exposed population is being migrated to TB exposed class at the rate $q(1-p)S(t)$.

Further, the TB patients are being caught COVID-19 infection at rate $(1-q)(1-p)S(t)$. τ and γ are the progression rates of TB exposed to infectious class I and COVID-19 compartmental, respectively. The relationship between these biological parameters is explicated stated in the model (see Table 1).

Assumption

(i) The total population size $S + E_H + E_C + I + R = N$ is supposed to be constant throughout the study.

(ii) All the rates are supposed to be constant.

(iii) The migration factor has negligible effects on tuberculosis diseases.

Table 1
State variables description.

State Variables	Description
S	Susceptible Individuals.
E_H	Exposed TB Individuals.
E_C	Exposed COVID-19 Individuals.
I	Infected Individuals.
R	Recovered Individuals.

3. Properties of the model

In this section, we discuss some preliminary properties of the proposed model, which are useful in finding the existence and uniqueness of the solution.

Uniqueness of Solution for the Model

The general first order ODE in the form

$$x' = g(x,t), \quad x(0) = x_0 \tag{2}$$

One will be interested in asking the following equations:

(a) Under what conditions, the solution of Eq. (2) exists?

(b) Under what conditions, there is a unique solution to the equation (2) ?

To answer these, let

$$g_1 = \Omega - \left(\frac{\alpha I}{N} + \mu\right)S + f\phi E_H,$$
$$g_2 = \frac{\alpha I}{N}q(1-p)S - (\mu+\tau)E_H - \phi E_H,$$
$$g_3 = \frac{\alpha I}{N}(1-q)(1-p)S - (\mu+\gamma)E_C,$$
$$g_4 = \tau E_H + \gamma E_C + \frac{\alpha I}{N}pS - (\mu+d+r)I + (1-f)\phi E_H,$$
$$g_5 = rI - \mu R.$$

We use the following theorem to establish the existence and uniqueness of the solution for our model.

Uniqueness of Solution

Theorem 3.1. *Let D be the domain,*

$$|t - t_0| \le c, \|y - y_0\| \le d, \tag{3}$$

where $y = (y_1, y_2, \dots, y_n), y_0 = (y_{10}, y_{20}, \dots, y_{n0})$, and $g(t,x)$ satisfies the Lipschitz condition:

$$\|g(t,y_1) - g(t,y_2)\| \le M\|y_1 - y_2\|. \tag{4}$$

Then, the ordered pairs (t,y_1) and (t,y_2) are in the domain D, where $M \ge 0$, there exist a positive constant δ and a unique continuous vector solution $y(t)$ of system (1) in the interval $|t - t_0| \le \delta$. It is important to note that condition (2) is satisfied by $\left\{\frac{\partial g_i}{\partial y_j} : i,j = 1,2,3,\dots,n\right\}$ is continuous and bounded in the domain D.

If $g(t,y)$ is a continuous partial derivative $\frac{\partial g_i}{\partial y_j}$ on a bounded closed convex domain U, where U is the real number, then it satisfies Lipschitz condition in U.

Our interest in the domain that is $\aleph \in [1,U]$. Thus, we look for a bounded solution $U > 0$. Then, we prove the below existence theorem.

Existence of Solution

Theorem 3.2. *Let D be the domain defined in equation such that (2) and (3) hold. Then, there exist a solution of the system (1) which is bounded in the domain D.*

Proof. Let

$$g_1 = \Omega - \left(\frac{\alpha I}{N} + \mu\right)S + f\phi E_H,$$
$$g_2 = \frac{\alpha I}{N}q(1-p)S - (\mu+\tau)E_H - \phi E_H,$$
$$g_3 = \frac{\alpha I}{N}(1-q)(1-p)S - (\mu+\gamma)E_C,$$
$$g_4 = \tau E_H + \gamma E_C + \frac{\alpha I}{N}pS - (\mu+d+r)I + (1-f)\phi E_H,$$
$$g_5 = rI - \mu R.$$

We show that $\left\{\frac{\partial g_i}{\partial y_j} : i,j = 1,2,3,4,5\right\}$ are continuous as well as bounded. We will find the following partial derivatives for all equations of the system (1).

$\left|\frac{\partial g_1}{\partial S}\right| = \left|-\left(\frac{\alpha I}{N} + \mu\right)\right| < \infty, \left|\frac{\partial g_1}{\partial E_H}\right| = |f\phi| < \infty, \left|\frac{\partial g_1}{\partial E_C}\right| = |0| < \infty, \left|\frac{\partial g_1}{\partial I}\right| = \left|\frac{\alpha S}{N}\right| < \infty, \left|\frac{\partial g_1}{\partial R}\right| = |0| < \infty,$

$\left|\frac{\partial g_2}{\partial S}\right| = \left|\frac{\alpha I}{N}q(1-p)\right| < \infty, \left|\frac{\partial g_2}{\partial E_H}\right| = |-(\mu+\tau+\phi)| < \infty, \left|\frac{\partial g_2}{\partial E_C}\right| = |0| < \infty, \left|\frac{\partial g_2}{\partial I}\right| = \left|\frac{\alpha I}{N}q(1-p)S\right| < \infty, \left|\frac{\partial g_2}{\partial R}\right| = |0| < \infty,$

$\left|\frac{\partial g_3}{\partial S}\right| = \left|\frac{\alpha I}{N}(1-q)(1-p)\right| < \infty, \left|\frac{\partial g_3}{\partial E_H}\right| = |0| < \infty, \left|\frac{\partial g_3}{\partial E_C}\right| = |-(\mu+\gamma)| < \infty, \left|\frac{\partial g_3}{\partial I}\right| = \left|\frac{\alpha}{N}(1-q)(1-p)S\right| < \infty, \left|\frac{\partial g_3}{\partial R}\right| = |0| < \infty,$

$\left|\frac{\partial g_4}{\partial S}\right| = \left|-\frac{\alpha I}{N}p\right| < \infty, \left|\frac{\partial g_4}{\partial E_H}\right| = |\tau + (1-f)\phi| < \infty, \left|\frac{\partial g_4}{\partial E_C}\right| = |\gamma| < \infty, \left|\frac{\partial g_4}{\partial I}\right| =$
$\left|-\frac{\alpha}{N}pS - (\mu+d+r)\right| < \infty, \left|\frac{\partial g_4}{\partial R}\right| = |0| < \infty,$

$\left|\frac{\partial g_5}{\partial S}\right| = |0| < \infty, \left|\frac{\partial g_5}{\partial E_H}\right| = |0| < \infty, \left|\frac{\partial g_5}{\partial E_C}\right| = |0| < \infty, \left|\frac{\partial g_5}{\partial I}\right| = |r| < \infty, \left|\frac{\partial g_5}{\partial R}\right| = |-\mu| < \infty.$

We have established that these twenty-five partial derivatives are continuous as well as bounded hence, theorem (2), yields that there exists a unique solution of the system (1) in the domain D.

3.1. Invariant region and attractively

The dynamical transmission of the system (1) will be analyzed in the below biological feasible region, $\Xi \subset R_+^5$ in which $\Xi = \left\{(S,E_H,E_C,I,R) \in R_+^5; S > 0, E_H \ge 0, E_C \ge 0, I \ge 0, R \ge 0 : S + E_H + E_C + I + R \le \frac{\Omega}{\mu}\right\}$.

Theorem 3.3. *The biological feasible region $\Xi \subset R_+^5$ is positively invariant for the system (1) with respect to ICs in R_+^5.*

Proof. We have

$$N = S + E_H + E_C + I + R, \tag{5}$$
$$\frac{dN}{dt} \le \Omega - \mu N - dI,$$
$$\lim_{t\to\infty} N(t) \le \frac{\Omega}{\mu}.$$

Now, let us discuss the solution of Eq. (5) and we get

$$N(t) \le N(0)e^{\mu t} + \frac{\Omega}{\mu}\left(1 - e^{-\mu t}\right).$$

Therefore, for positive value of t, $N(t)$ converges to infinity. So, the solutions of the system (1) with ICs Ξ remain in Ξ. Thus, the biological feasible region Ξ is positively invariant and attracts all the solutions in R_+^5.

3.2. Positively and boundedness

Theorem 3.4. *The solution of the system (1) is positively bounded for all $(S(0), E_H(0), E_C(0), I(0), R(0)) \in R_+^5$ and also define for the positive value of time t.*

Proof. In order to demonstrate the positive solution, it is required to verify that on every hyperplane bounding the positive orhant, the

vector field point R_+^5. From the system (1), we have,

$$\frac{dS}{dt}(at\ S=0)=\Omega+f\phi E_H\geq 0,$$
$$\frac{dE_H}{dt}(at\ E_H=0)=\frac{\alpha I}{N}q(1-p)S\geq 0,$$
$$\frac{dE_C}{dt}(at\ E_C=0)=\frac{\alpha I}{N}(1-q)(1-p)S\geq 0,$$
$$\frac{dI}{dt}(at\ I=0)=\tau E_H+\gamma E_C+\frac{\alpha I}{N}pS+(1-f)\phi E_H\geq 0,$$
$$\frac{dR}{dt}(at\ R=0)=rI\geq 0.$$

Thus, the solution obtained from the above set problem will remains in R_+^5, and thus we have the following bounded feasible region.

$\Xi = \{ (S(0), E_H(0), E_C(0), I(0), R(0)) \in R_+^5; (S(0), E_H(0), E_C(0), I(0), R(0)) \geq 0 \}$.

4. The analysis

In this section, the model analysis is achieved by measuring the points of equilibrium.

4.1. Existence of steady state of the system

The critical points are obtained by taking all the five equations of the system (1) equal to zero, this means, $\frac{dS}{dt}=\frac{dE_H}{dt}=\frac{dE_C}{dt}=\frac{dI}{dt}=\frac{dR}{dt}=0$. The disease-free critical point is the position where there is no infection in the class. Next, solving the disease-free critical points the first equation of the system (1) yields $S=\frac{\Omega}{\mu}$ and from second equation of the system (1) we have $E_H=0$ and from third equation of the system (1) we get $E_C=0$ and from fourth equation of the system (1) we have $I=0$ and from last equation of the system (1) we obtained $R=0$. Thus, the disease free critical point $\gamma=0$ is $\gamma_0=\left(\frac{\Omega}{\mu},0,0,0,0\right)$.

4.2. Endemic equilibrium point

This is the position where the disease persists in the system. Therefore, the system (1) has an endemic critical point $E_1=(S^*,E_H^*,E_C^*,I^*,R^*)$. Thus, we solve the system (1) for S^*,E_H^*,E_C^*,I^*,R^*. Hence from the first equation of system (1), we obtained

$$S^*=\frac{(\mu+\tau+\phi)\Omega}{(\mu+\tau+\phi)(\beta^*+\mu)-\beta^* f\phi q(1-p)}, \tag{6}$$
$$E_H^*=\frac{\beta^*\Omega q(1-p)}{(\mu+\tau+\phi)(\beta^*+\mu)-\beta^* f\phi q(1-p)}, \tag{7}$$
$$E_C^*=\frac{\Omega\beta^*(\mu+\tau+\phi)(1-q)(1-p)}{(\mu+\gamma)[(\mu+\tau+\phi)(\beta^*+\mu)-\beta^* f\phi q(1-p)]}. \tag{8}$$

Hence,

$$I^*=\frac{\alpha\Omega[C_1+C_2+C_3-N\mu(\mu+\tau+\phi)C_4]}{\alpha(\mu+\gamma)(\mu+d+r)[(\mu+\tau+\phi)-f\phi q(1-p)]}, \tag{9}$$

where $C_1=\tau q(\mu+\gamma)(1-p), C_2=\gamma(1-q)(1-p)(\mu+\tau), C_3=-P(\mu+\gamma)(\mu+\tau+\phi), C_4=(\mu+\gamma)(\mu+d+r)$ and

$$R^*=\frac{\frac{\alpha\Omega[(\mu+\gamma)\tau q(1-p)+\gamma(1-q)(1-p)(\mu+\tau)}{-(\mu+\gamma)p(\mu+\tau+\phi)]}}{\mu(\mu+\gamma)(\mu+d+r)(\beta^*+\mu)}. \tag{10}$$

Since, $\beta^*=\frac{\alpha I^*}{N^*}$ substituting Eq. (9) into $\beta^*=\frac{\alpha I^*}{N^*}$, we have

$$\beta^*=\frac{\alpha[\alpha\Omega(C_1+C_2+C_3)-N\mu(\mu+\tau+\phi)C_4]}{N^*\alpha C_4[(\mu+\tau+\phi)-f\phi q(1-p)]}.$$

For the case when $\beta^*=0$ in equations (6) to (10), the endemic equilibrium point is

$$E_1=(S^*,E_H^*,E_C^*,I^*,R^*)=\left(\frac{\Omega}{\mu},0,0,0,0\right).$$

Now, the endemic critical point is in terms of the force of infection β^*. On substituting $N^*\beta^*=\alpha I^*$, we have

$$I^*=\frac{\alpha N^*(B_3+B_4+bc)-abc}{\alpha(B_1+B_2+B_3+B_4+B_5+B_6+bc+ba)}$$

since $N^*=S^*+E_H^*+E_C^*+I^*+R^*$. Thus,

$$I^*=\frac{\alpha(S^*+E_H^*+E_C^*+I^*+R^*)(B_3+B_4+bc)-abc}{\alpha(B_1+B_2+B_3+B_4+B_5+B_6+bc+ba)},$$

where $B_1=qac(1-p), B_2=bd(1-q)(1-p), B_3=c\tau q(1-p), B_4=d\gamma(1-q)(1-p), B_5=c\tau q(1-p), B_6=d\gamma(1-q)(1-p)$, and $a=\tau, b=\gamma, c=\mu+\gamma, d=\mu+\tau$. On substituting the equilibrium point in equation $(S^*,E_H^*,E_C^*,I^*,R^*)$, we obtain

$$H_1\beta^{*2}+H_2\beta^*-H_3=0, \tag{11}$$

where, $H_1=ZA\mu(\mu+\tau)(\mu+\gamma), H_2=(L_1-L_2-L_3-L_4-L_5), H_3=\alpha\pi\mu C_4(\mu+\tau)(\mu+\gamma)$, and $L_1=ZA\mu^2(\mu+\tau)(\mu+\gamma), L_2=\mu C_4q(1-p)(\mu+\tau), L_3=\mu C_4(1-q)(1-p)(\mu+\gamma), L_4=Z\mu C_4q(1-p)(\mu+\tau), L_5=r(C_1+C_2+C_3)(\mu+\tau)(\mu+\gamma)$. Also, $Z=[(\mu+\gamma)\tau q(1-p)+\gamma(1-q)(1-p)(\mu+\tau)-(\mu+\gamma)p(\mu+\tau+\phi)]$ and $A=\alpha(B_1+B_2+B_3+B_4+B_5+B_6+bc+ba)$. From the quadratic Eq. (11), we get

$$\beta^*=\frac{-H_2\pm\sqrt{H_2^2+4H_1H_3}}{2H_1}.$$

Thus, the above equation has one positive root when $\sqrt{H_2^2+4H_1H_3}>H_2$. So, it demonstrates that there exists at least one positive critical point.

4.3. Computation of basic reproduction number ($\mathcal{R}_0$)

By, the next generation matrix method [28], we evaluate the $\mathcal{R}_0$: $F^*=\begin{bmatrix}\frac{\alpha}{N}q(1-p)S\\ \frac{\alpha}{N}(1-q)(1-p)S\\ \frac{\alpha}{N}p\end{bmatrix}$, *and* $V^*=\begin{bmatrix}\mu+\tau+\phi\\ \mu+\gamma\\ -\tau-\gamma-(1-f)\phi\mu+d+r\end{bmatrix}$. The Jacobian matrices after taking the partial derivatives of F^* and V^* at E_0 are $F=\begin{bmatrix}0&0&\frac{\alpha}{N}q(1-p)S\\ 0&0&\frac{\alpha}{N}(1-q)(1-p)S\\ 0&0&\frac{\alpha}{N}p\end{bmatrix}$ *and*

$$V=\begin{bmatrix}\mu+\tau+\phi&0&0\\ 0&\mu+\gamma&0\\ -\tau-(1-f)\phi&-\gamma&\mu+d+r\end{bmatrix}$$

$|V|=(\mu+\gamma)(\mu+\tau+\phi)(\mu+d+r)$.

Now,

$$FV^{-1}==\begin{bmatrix}0&0&\frac{\alpha\Omega q(1-p)}{N\mu(\mu+d+r)}\\ 0&0&\frac{\alpha\Omega(1-q)(1-p)}{N\mu}\\ 0&0&\frac{\alpha}{N}p\end{bmatrix},$$

$$\mathcal{R}_0=\sqrt{\frac{\alpha\Omega q(1-p)}{N\mu(\mu+d+r)}}.$$

Thus, the $\mathcal{R}_0$ yields the average quantity of infected populations generated by the infected in a fully susceptible population and for our system (1). This yields by the above expression of $\mathcal{R}_0$ [28].

4.4. Local stability of disease free equilibrium point

Local stability of a critical point means that if we put the system somewhere nearby the point then it will move itself to the same point after some time. Now, we will discuss the local stability by computing

the Jacobian matrix as follow.

$$J=\begin{bmatrix} -\mu & \phi & 0 & -\frac{\alpha S}{N} & 0\\ 0 & (\mu+\tau+\phi) & 0 & \frac{\alpha}{N}q(1-p)S & 0\\ 0 & 0 & -(\mu+\gamma) & \frac{\alpha}{N}(1-q)(1-p)S & 0\\ 0 & \tau+(1-f) & \gamma & \frac{\alpha}{N}pS-(\mu+d+r) & 0\\ 0 & 0 & 0 & r & \mu \end{bmatrix}.$$

At $E_0=\left(\frac{\Omega}{\mu},0,0,0,0\right)$. Then,

$$J_{E_0}=\begin{bmatrix} -\mu & \phi & 0 & -\frac{\alpha\Omega}{N\mu} & 0\\ 0 & (\mu+\tau+\phi) & 0 & \frac{\alpha\Omega}{N\mu}q(1-p) & 0\\ 0 & 0 & -(\mu+\gamma) & \frac{\alpha\Omega}{N\mu}(1-q)(1-p) & 0\\ 0 & \tau+(1-f) & \gamma & \frac{\alpha\Omega}{N\mu}p-(\mu+d+r) & 0\\ 0 & 0 & 0 & r & \mu \end{bmatrix}.$$

We now use the transformation

$$S=V+\bar{S},E_H=W+\bar{E}_H,E_C=X+\bar{E}_C,I=Y+\bar{I},R=Z+\bar{R}$$

and then linearize the system $\begin{bmatrix}\dot{V}\\ \dot{W}\\ \dot{X}\\ \dot{Y}\\ \dot{Z}\end{bmatrix}=J_{E_0}\begin{bmatrix}V\\ W\\ X\\ Y\\ Z\end{bmatrix}$. We get the linearized system

$$\begin{aligned}
\dot{V}&=-\mu V+f\phi W-\frac{\alpha\Omega}{N\mu}Y,\\
\dot{W}&=-(\mu+\tau+\phi)W+\frac{\alpha\Omega}{N\mu}q(1-p)Y,\\
\dot{X}&=-(\mu+\gamma)X+\frac{\alpha\Omega}{N\mu}(1-q)(1-p)Y,\\
\dot{Y}&=\big(\tau+(1-f)\big)W+\gamma X+\left(\frac{\alpha\Omega}{N\mu}p-(\mu+d+r)\right)Y,\\
\dot{Z}&=rY+\mu Z.
\end{aligned}$$

Theorem 4.1. *The disease free equilibrium point* $\bar{E}\left(\frac{\Omega}{\mu},0,0,0,0\right)$ *is locally asymptotically stable if*

$$\begin{aligned}
&(a_1f\phi)^2<4a_1a_2\mu(\mu+\tau+\phi),\\
&\left(a_1\left(-\frac{\alpha\Omega}{N\mu}\right)\right)^2<4a_1a_2(-\mu)\left(\frac{\alpha\Omega}{N\mu}p-(\mu+d+r)\right),\\
&\left(a_2\left(\frac{\alpha\Omega}{N\mu}q(1-p)\right)\right)^2<4a_2^2\left(\frac{\alpha\Omega}{N\mu}p-(\mu+d+r)\right)\\
&\big(-(\mu+\tau+\phi)\big),\\
&\left(a_3\left(\frac{\alpha\Omega}{N\mu}(1-q)(1-p)\right)\right)^2<4a_2a_3\left(\frac{\alpha\Omega}{N\mu}p-(\mu+d+r)\right)\\
&\big(-(\mu+\gamma)\big),\\
&\left(a_4\big(\tau+(1-f)\big)\right)^2<4a_2^2\left(\frac{\alpha\Omega}{N\mu}p-(\mu+d+r)\right)\\
&\big(-(\mu+d+r)\big),\\
&\big(a_4\gamma\big)^2<4a_2a_3\left(\frac{\alpha\Omega}{N\mu}p-(\mu+d+r)\right)\big(-(\mu+\gamma)\big),\\
&\big(a_5r\big)^2<4a_2a_5\left(\frac{\alpha\Omega}{N\mu}p-(\mu+d+r)\right)\mu,
\end{aligned}$$

where, a_1,a_2,a_3,a_4,a_5 *are arbitrary constants.*

4.5. Global stability of disease free equilibrium points

The global stability of disease free equilibrium points id given in the form of theorem as below:

Theorem 4.2. *The disease free equilibrium point* $\bar{E}\left(\frac{\Omega}{\mu},0,0,0,0\right)$ *is globally asymptotically stable if the Lyapunov function* $V_1=\frac{1}{2}a_1V^2+\frac{1}{2}a_2W^2+\frac{1}{2}a_3X^2+\frac{1}{2}a_4Y^2+\frac{1}{2}a_5Z^2$ *is negative definite.*

Proof. See Appendix A.

4.6. Local stability of endemic equilibrium points

In this subsection, we evaluated the local asymptotically Stability of endemic equilibrium points. At $E^*=\big(S^*,E_H^*,E_C^*,I^*,R^*\big)$. Then, the variational matrix J_{E^*} is given as follows:

$$=\begin{bmatrix} -\mu & \phi & 0 & -\frac{\alpha}{N}S^* & 0\\ 0 & (\mu+\tau+\phi) & 0 & \frac{\alpha}{N}q(1-p)S^* & 0\\ 0 & 0 & -(\mu+\gamma) & \frac{\alpha}{N}(1-q)(1-p)S^* & 0\\ 0 & \tau+(1-f) & \gamma & \frac{\alpha}{N}pS^*-(\mu+d+r) & 0\\ 0 & 0 & 0 & r & \mu \end{bmatrix}.$$

We now use the transformation

$$S=P+S^*,E_H=Q+E_H^*,E_C=R+E_C^*,I=S+I^*,$$

$R=T+R^*$ and then linearize the system $\begin{bmatrix}\dot{P}\\ \dot{Q}\\ \dot{R}\\ \dot{S}\\ \dot{T}\end{bmatrix}=J_{E^*}\begin{bmatrix}P\\ Q\\ R\\ S\\ T\end{bmatrix}$.

We get the linearized system

$$\begin{aligned}
\dot{P}&=-\mu P+f\phi Q-\frac{\alpha}{N}S^*S,\\
\dot{Q}&=-(\mu+\tau+\phi)Q+\frac{\alpha}{N}q(1-p)S^*S,\\
\dot{R}&=-(\mu+\gamma)R+\frac{\alpha}{N}(1-q)(1-p)S^*S,\\
\dot{S}&=\big(\tau+(1-f)\big)Q+\gamma R+\left(\frac{\alpha}{N}pS^*-(\mu+d+r)\right)S,\\
\dot{T}&=rS+\mu T.
\end{aligned}$$

Theorem 4.3. *The endemic equilibrium point* $E^*\big(S^*,E_H^*,E_C^*,I,R\big)$ *is locally asymptotically stable if*

$$\begin{aligned}
&(b_1f\phi)^2<4b_1b_2\mu(\mu+\tau+\phi),\\
&\left(b_1\left(-\frac{\alpha}{N}S^*\right)\right)^2<4b_1b_2(-\mu)\left(\frac{\alpha}{N}pS^*-(\mu+d+r)\right),\\
&\left(b_2\left(\frac{\alpha}{N}q(1-p)S^*\right)\right)^2<4b_2^2\left(\frac{\alpha}{N}pS^*-(\mu+d+r)\right)\\
&\big(-(\mu+\tau+\phi)\big),\\
&\left(b_3\left(\frac{\alpha}{N}(1-q)(1-p)S^*\right)\right)^2<4b_2b_3\left(\frac{\alpha}{N}pS^*-(\mu+d+r)\right)\\
&\big(-(\mu+\gamma)\big),\\
&\left(b_4\big(\tau+(1-f)\big)\right)^2<4b_2^2\left(\frac{\alpha}{N}pS^*-(\mu+d+r)\right)\big(-(\mu+d+r)\big),\\
&\big(b_4\gamma\big)^2<4b_2b_3\left(\frac{\alpha}{N}pS^*-(\mu+d+r)\right)\big(-(\mu+\gamma)\big),\\
&\big(b_5r\big)^2<4b_2b_5\left(\frac{\alpha}{N}pS^*-(\mu+d+r)\right)\mu,
\end{aligned}$$

where, b_1,b_2,b_3,b_4,b_5 *are arbitrary constants.*

4.7. Global stability of endemic equilibrium points

In this subsection, we present the global asymptotically stability of endemic equilibrium points $E^*\big(S^*,E_H^*,E_C^*,I,R\big)$ which is given in the form of theorem as follows:

Theorem 4.4. *The endemic equilibrium point* $E^*(S^*, E_H^*, E_C^*, I, R)$ *is globally asymptotically stable if the Lyapunov function* $V_2 = \frac{1}{2}b_1P^2 + \frac{1}{2}b_2Q^2 + \frac{1}{2}b_3R^2 + \frac{1}{2}b_4S^2 + \frac{1}{2}b_5T^2$ *is negative definite.*

Proof. See Appendix B.

5. Optimal control

We have used the optimal control theory as a powerful tool to understand the ways to reduce the COVID-19 spread the worked by devising disease intervention strategies. We consider many important issues pertaining to TB and COVID-19 infection that have not yet been adequately addressed in the literature earlier. The proposed mathematical model enables the application of optimal control theory to assess containment scenarios while maintaining the response capability of health scenarios. Since the pandemic has shown that public health is more than a treatment issue as it also affects the entire society.

5.1. Existence of optimal control model

COVID-19 is spread by a host contact with the infected population, we find the best optimal control strategies while keeping the following essential constraints in mind.

(1) u_1 is the number of exposed individuals with COVID-19 infection get vaccinated, so that no more infection can spread.

(2) u_2 the number of COVID-19 infected people be quarantined.

(3) u_3 is the number of both COVID-19 and TB infection individuals be quarantined.

$$F(l_i, \Xi) = \int_0^T \left(W_1S^2 + W_2E_H^2 + W_3E_C^2 + W_4I^2 + W_5R^2 + u_1l_1^2 + u_2l_2^2 + u_3l_3^2\right)dt, \tag{12}$$

where, Ξ is the set of all compartmental variables, W_1, W_2, W_3, W_4, W_5 are the non-negative weight constants for the state variable S, E_H, E_C, I, R, respectively.

Now, we will find every value of control variable l_1, l_2, l_3 from the initial value of base 0 to final value T and we have

$$F(l_i(t)) = min\left\{\frac{F(l_i^*, \Xi)}{l_i} \in M\right\}, i = 1, 2, 3$$

where, M is the smooth function for the interval $[0, 1]$.

Thus, the Lagrangian function is related to objective function and is given by

$$\begin{aligned}\Gamma(\Xi, W_i) =& W_1S^2 + W_2E_H^2 + W_3E_C^2 + W_4I^2 + W_5R^2 + u_1l_1^2 \\ &+u_2l_2^2 + u_3l_3^2 \\ &+\lambda_1\left(\Omega - \left(\frac{\alpha I}{N} + \mu\right)S + f\phi E_H\right) \\ &+\lambda_2\left(\frac{\alpha I}{N}q(1-p)S - (\mu+\tau)E_H - \phi E_H\right) \\ &+\lambda_3\left(\frac{\alpha I}{N}(1-q)(1-p)S - (\mu+\gamma)E_C\right) \\ &+\lambda_4\left(\tau E_H + \gamma E_C + \frac{\alpha I}{N}pS - (\mu+d+r)I\right. \\ &\left.+(1-f)\phi E_H\right) + \lambda_5\left(rI - \mu R\right).\end{aligned}$$

The adjoint equation variables, $\lambda_i = (\lambda_1, \lambda_2, \lambda_3, \lambda_4, \lambda_5)$ for the system (1) is calculated by taking the partial derivative of Γ with respect to each state variable S, E_H, E_C, I, R, we have

$$\begin{aligned}\dot{\lambda}_1 =& -2W_1S(\lambda_1 - \lambda_4 p)\frac{\alpha I}{N} - (\lambda_2 q + \lambda_3(1-q))\frac{\alpha I}{N} + \lambda_1\mu, \\ \dot{\lambda}_2 =& -2W_2E_H - \lambda_1 f\phi + \lambda_2(\mu+\tau+\phi) - \lambda_4(\tau + (1-f)\phi) \\ &+(\lambda_3 - \lambda_2) + u_1(\lambda_1 - \lambda_4)u_2, \\ \dot{\lambda}_3 =& -2W_3E_C + (\lambda_3 - \lambda_4)\gamma + \lambda_3\gamma, \\ \dot{\lambda}_4 =& -2W_4I + \lambda_1\frac{\alpha}{N}S - \lambda_2\frac{\alpha}{N}q(1-p)S - \lambda_3\frac{\alpha}{N}(1-q)(1-p)S \\ &+\lambda_4(\mu+d+r) - \lambda_5 r + (\lambda_4 - \lambda_3)u_3, \\ \dot{\lambda}_5 =& -2W_5R + \lambda_5\mu.\end{aligned}$$

Hence, the above work gives us,

$$\begin{aligned}l_1^* &= max\left(c_1, min\left(d_1, \frac{E_H(\lambda_3 - \lambda_2)u_1}{2u_1}\right)\right), \\ l_2^* &= max\left(c_2, min\left(d_2, \frac{E_C(\lambda_2 - \lambda_4)u_2}{2u_2}\right)\right), \\ l_3^* &= max\left(c_3, min\left(d_3, \frac{I(\lambda_4 - \lambda_3)u_3}{2u_3}\right)\right).\end{aligned}$$

6. Bifurcation analysis

Bifurcation analysis in dynamical systems means a small change in bifurcation parameters leads to a sudden qualitative change in the system behaviour. Generally, at a bifurcation junction, properties of equilibrium points and periodic orbits changes. The region of stable solutions can be determined by computing stability boundaries directly as functions of the relevant system parameters. For the sake of convenience, we will take $S = z_1, E_H = z_2, E_C = z_3, I = z_4, R = z_5$. Since, by the vector notation $Z = (z_1, z_2, z_3, z_4, z_5)^T$, the dynamical system (1) can be expressed in the form as below:

$$\frac{dZ}{dt} = (z_1, z_2, z_3, z_4, z_5)^T$$

where,

$$\begin{aligned}z_1' =& \Omega - \left(\frac{\alpha I}{N} + \mu\right)S + f\phi E_H, \\ z_2' =& \frac{\alpha I}{N}q(1-p)S - (\mu+\tau)E_H - \phi E_H, \\ z_3' =& \frac{\alpha I}{N}(1-q)(1-p)S - (\mu+\gamma)E_C, \\ z_4' =& \tau E_H + \gamma E_C + \frac{\alpha I}{N}pS - (\mu+d+r)I + (1-f)\phi E_H, \\ z_5' =& rI - \mu R.\end{aligned} \tag{13}$$

The Jacobian matrix of $z_i (i = 1, 2, 3, 4, 5)$ at DFE is evaluated as:

$$J_{\alpha^*} = \begin{bmatrix} -\mu & \phi & 0 & -\frac{\alpha\Omega}{N\mu} & 0 \\ 0 & (\mu+\tau+\phi) & 0 & \frac{\alpha\Omega}{N\mu}q(1-p) & 0 \\ 0 & 0 & -(\mu+\gamma) & \frac{\alpha\Omega}{N\mu}(1-q)(1-p) & 0 \\ 0 & \tau+(1-f) & \gamma & \frac{\alpha\Omega}{N\mu}p - (\mu+d+r) & 0 \\ 0 & 0 & 0 & r & \mu \end{bmatrix}.$$

Now, consider the case when the $\mathcal{R}_0$ is equal to unity, then we will take $\alpha = \alpha^*$ as the bifurcation parameter. Solving for this parameter from the $\mathcal{R}_0$ which is equal to unity yields $\alpha = \alpha^* = \sqrt{\frac{\alpha\Omega q(1-p)}{N\mu(\mu+d+r)}}$. Therefore, by using the [29], we will be able to find whether or not the system (12) demonstrate the backward bifurcation at basic reproduction number at unity.

Theorem 6.1. *Suppose the following general system of ODE with parameter* ϕ, $\frac{dZ}{dt} = h(z, \varphi)$ $h : R^n \times R \to R, h \in C^2(R^n \times R), h(z, \varphi) \equiv 0$, *for all* φ *and* $z = 0$,

(a) $B = D_z h(0, 0) = \left(\frac{\partial h_i}{\partial z_j}(0, 0)\right)$ *is a linear matrix of system (13) around the critical point zero with h evaluated at zero,*

(b) $z = 0$ *is the simple characteristic value of B and other characteristic values of B have negative real parts.*

Suppose, h_p *be the* p*th part of h and* $c = \sum_{p,q=1}^{m} u_p u_q \frac{\partial^2 h_p}{\partial z_p \partial z_q}(0, 0)$, *then the local dynamical system around the critical point zero is fully determined by the signs of c. Particularly, if* $c > 0$, *then a backward Hopf-type bifurcation occurs at* φ *equal to zero.*

Table 2
Biological parametric description along with their values.

Parameter	Description	Parametric values	Sources
μ	Natural death rate	0.00987	[7]
α	Infection contact rate	0.5	Assumed
p	Fraction of fast progresses to the active disease	0.35	[30]
$1-p$	Fraction of susceptible class to latent tuberculosis	0.65	[30]
q	Fraction of susceptible class to latent tuberculosis	0.83	[30]
$1-q$	Fraction of susceptible class to latent COVID-19	0.917	[30]
$q(1-p)$	Fraction of susceptible population of susceptible class to host TB after mix up with susceptible class to infected population $(1-p)$	0.053	[30]
$(1-q)(1-p)$	Fraction of susceptible class to exposed COVID-19 after adjustment with susceptible to infected population	0.596	[30]
τ	Indicate the progression rate from exposed TB to infectious population	0.0016	Assumed
γ	Indicates the progression rate from exposed COVID-19 to infectious population	0.0001	Assumed
r	Recovery rate	0.85	[22]
d	TB induced death rate	0.00013	[7]
f	Vaccination rate	0.7	[11]
$1-f$	Fraction of remaining TB vaccinated population	0.3	[11]
ϕ	COVID-19 induced mortality rate	0.1	[11]

6.1. Computation of characteristic values of J^*_α

It is easily observed that the Jacobian with $\alpha = \alpha^*$ of the linearized system has a simple zero characteristic value and all other characteristic values have negative real parts. Thus, center manifold theory may be applied to analyse the dynamical system (12) near $\alpha = \alpha^*$. At the point when basic reproduction number is equal to unity, this can be demonstrated that the matrix J^*_α has a right characteristic vector that are given by $u = [u_1, u_2, u_3, u_4, u_5]^T$ where $u_1 = \frac{f\phi N\mu+\alpha\Omega}{N\mu^2}, u_2 = q(1-p)\frac{\alpha\Omega}{N\mu(\mu+d+\phi)}, u_3 = (1-q)(1-p)\frac{\alpha\Omega}{N\gamma(\mu+\gamma)}, u_4 = \frac{\tau+\gamma+(1-f)\phi}{\mu+d+r}$ *and* $u_5 = \frac{r}{\mu}$.

7. Sensitivity analysis

In epidemiology, sensitivity analysis may be used to determine the impact of an unmeasured dose on the casual finding of a sample. The use of sensitivity analysis in mathematical modelling of infectious disease is suggested in the coronavirus disease 2019 outbreak [31–37]. In model (1), we use three key biological parameters, namely as α, q *and* $(1-p)$, which significantly affect the basic reproduction number $\mathcal{R}_0$ [38]. The sensitivity of $\mathcal{R}_0$ to the change of these biological parameters is represented by the partial derivative listed below:

$$\begin{aligned}
\frac{\partial\mathcal{R}_0}{\partial\alpha} &= \frac{1}{2\sqrt{\mathcal{R}_0}}\times\frac{\alpha(1-p)\Omega}{N\gamma(\mu+d+r)},\\
\frac{\partial\mathcal{R}_0}{\partial q} &= \frac{1}{2\sqrt{\mathcal{R}_0}}\times\frac{q(1-p)\Omega}{N\gamma(\mu+d+r)},\\
\frac{\partial\mathcal{R}_0}{\partial(1-p)} &= \frac{1}{2\sqrt{\mathcal{R}_0}}\times\frac{\alpha q\Omega}{N\gamma(\mu+d+r)}.
\end{aligned} \tag{14}$$

Since all the calculated partial derivatives are non-negative, we conclude that $\mathcal{R}_0$ increases with the increase of any parameter given above. To know the effect of corresponding changes to these parameters on $\mathcal{R}_0$, we will calculate elasticities since elasticity is nothing but the corresponding responses to a corresponding perturbation.

$$\begin{aligned}
E_\alpha &= \frac{\alpha}{\mathcal{R}_0}\times\frac{\partial\mathcal{R}_0}{\partial\alpha} = \frac{\alpha}{\mathcal{R}_0}\times\frac{1}{2\sqrt{\mathcal{R}_0}}\times\frac{\alpha(1-p)\Omega}{N\gamma(\mu+d+r)},\\
E_q &= \frac{q}{\mathcal{R}_0}\times\frac{\partial\mathcal{R}_0}{\partial q} = \frac{q}{\mathcal{R}_0}\times\frac{1}{2\sqrt{\mathcal{R}_0}}\times\frac{q(1-p)\Omega}{N\gamma(\mu+d+r)},\\
E_{1-p} &= \frac{1-p}{\mathcal{R}_0}\times\frac{\partial\mathcal{R}_0}{\partial(1-p)} = \frac{1-p}{\mathcal{R}_0}\times\frac{1}{2\sqrt{\mathcal{R}_0}}\times\frac{\alpha q\Omega}{N\gamma(\mu+d+r)}.
\end{aligned}$$

From the Eq. (14), we observe that minor changes in q and $(1-p)$ have same result on $\mathcal{R}_0$. We also observe that $E_\alpha > E_q = E_{(1-p)}$ if $\sqrt{(\mathcal{R}_0)} < \frac{2\alpha}{\mu}$ and in this case minor change in α have a great effect on $\mathcal{R}_0$ compared to same corresponding changes in other biological parameters. Biologically it means that infection rate has larger effects on disease dynamics. The impact of these biological parameters on $\mathcal{R}_0$ is shown in Fig. 17.

8. Numerical simulation

In this section, we simulate the proposed mathematical model (1) by simulating various biological parameters given in Table 2. We use the default set of parameters cited in the literature and compute those values which are not found in the literature. In order to assess the impacts of various rates of TB cases and COVID-19 on the different populations, we simulate α, f, ϕ, q, τ and R parameters to see how these parameters affect the transmission dynamics of both diseases. In order to demonstrate this co-infection numerically via Runge–Kutta Method of fourth order. This numerical method is given as below:

$$y_{z+1} = y_z + \frac{1}{6}\left(k_1 + 2k_2 + 2k_3 + k_4\right). \tag{15}$$

where,

$$\begin{aligned}
k_1 &= hg(x_z, y_z),\\
k_2 &= hg\left(x_z + \frac{1}{2}d_k, y_z + \frac{1}{2}k_1\right),\\
k_3 &= hg\left(x_z + \frac{1}{2}d_k, y_z + \frac{1}{2}k_2\right),\\
k_4 &= hg\left(x_z + d_k, y_z + k_3\right).
\end{aligned}$$

Further,

$$\begin{aligned}
\frac{dS}{dt} &= g_1(t, S, E_H, E_C, I, R) = \Omega - \left(\frac{\alpha I}{N} + \mu\right)S + f\phi E_H,\\
\frac{dE_H}{dt} &= g_2(t, S, E_H, E_C, I, R) = \frac{\alpha I}{N}q(1-p)S - (\mu+\tau)E_H - \phi E_H,
\end{aligned}$$

$$\frac{dE_C}{dt} = g_3(t,S,E_H,E_C,I,R) = \frac{\alpha I}{N}(1-q)(1-p)S - (\mu+\gamma)E_C,$$
$$\frac{dI}{dt} = g_4(t,S,E_H,E_C,I,R) = \tau E_H + \gamma E_C + \frac{\alpha I}{N}pS - (\mu+d+r)I + (1-f)\phi E_H,$$
$$\frac{dR}{dt} = g_5(t,S,E_H,E_C,I,R) = rI - \mu R. \tag{16}$$

The Eq. (16) is solved by applying Runge–Kutta Method of fourth order based on algorithm given in Eq. (15). Hence, the system is given as follow:

$$\begin{aligned}
a_{z+2} &= a_{z+1} + \frac{1}{6}(k_1+2k_2+2k_3+k_4)d_k,\\
a_{z+3} &= a_{z+2} + \frac{1}{6}(l_1+2l_2+2l_3+l_4)d_k,\\
a_{z+4} &= a_{z+3} + \frac{1}{6}(m_1+2m_2+2m_3+m_4)d_k,\\
a_{z+5} &= a_{z+4} + \frac{1}{6}(n_1+2n_2+2n_3+n_4)d_k,\\
a_{z+6} &= a_{z+5} + \frac{1}{6}(p_1+2p_2+2p_3+p_4)d_k,
\end{aligned} \tag{17}$$

with step size d_k, we have

$$\begin{aligned}
k_1 &= \Omega - \left(\frac{\alpha I}{N}+\mu\right)S + f\phi E_H,\\
l_1 &= \frac{\alpha I}{N}q(1-p)S - (\mu+\tau)E_H - \phi E_H,\\
m_1 &= \frac{\alpha I}{N}(1-q)(1-p)S - (\mu+\gamma)E_C,\\
n_1 &= \tau E_H + \gamma E_C + \frac{\alpha I}{N}pS - (\mu+d+r)I + (1-f)\phi E_H,\\
p_1 &= rI - \mu R,
\end{aligned}$$

$$\begin{aligned}
k_2 &= \Omega - \left(\frac{\alpha}{N}\left(a_{z+1}+\frac{n_1d_k}{2}\right)+\mu\right)\left(a_{z+1}+\frac{k_1d_k}{2}\right) + f\phi\left(a_{z+1}+\frac{l_1d_k}{2}\right),\\
l_2 &= \frac{\alpha}{N}\left(a_{z+1}+\frac{n_1d_k}{2}\right)q(1-p)\left(a_{z+1}+\frac{k_1d_k}{2}\right) - (\mu+\tau+\phi)\left(a_{z+1}+\frac{l_1d_k}{2}\right),\\
m_2 &= \frac{\alpha}{N}\left(a_{z+1}+\frac{n_1d_k}{2}\right)(1-q)(1-p)\left(a_{z+1}+\frac{k_1d_k}{2}\right) - (\mu+\gamma)\left(a_{z+1}+\frac{m_1d_k}{2}\right),\\
n_2 &= \tau\left(a_{z+1}+\frac{l_1d_k}{2}\right) + \gamma\left(a_{z+1}+\frac{m_1d_k}{2}\right) + \frac{\alpha}{N}\left(a_{z+1}+\frac{n_1d_k}{2}\right)p\left(a_{z+1}+\frac{k_1d_k}{2}\right)\\
&\quad - (\mu+d+r)\left(a_{z+1}+\frac{n_1d_k}{2}\right) + (1-f)\phi\left(a_{z+1}+\frac{l_1d_k}{2}\right),\\
p_2 &= r\left(a_{z+1}+\frac{n_1d_k}{2}\right) - \mu\left(a_{z+1}+\frac{p_1d_k}{2}\right),\\
k_3 &= \Omega - \left(\frac{\alpha}{N}\left(a_{z+1}+\frac{n_2d_k}{2}\right)+\mu\right)\left(a_{z+1}+\frac{k_2d_k}{2}\right) + f\phi\left(a_{z+1}+\frac{l_2d_k}{2}\right),\\
l_3 &= \frac{\alpha}{N}\left(a_{z+1}+\frac{n_2d_k}{2}\right)q(1-p)\left(a_{z+1}+\frac{k_2d_k}{2}\right) - (\mu+\tau+\phi)\left(a_{z+1}+\frac{l_2d_k}{2}\right),\\
m_3 &= \frac{\alpha}{N}\left(a_{z+1}+\frac{n_2d_k}{2}\right)(1-q)(1-p)\left(a_{z+1}+\frac{k_2d_k}{2}\right) - (\mu+\gamma)\left(a_{z+1}+\frac{m_2d_k}{2}\right),\\
n_3 &= \tau\left(a_{z+1}+\frac{l_2d_k}{2}\right) + \gamma\left(a_{z+1}+\frac{m_2d_k}{2}\right)\\
&\quad + \frac{\alpha}{N}\left(a_{z+1}+\frac{n_2d_k}{2}\right)p\left(a_{z+1}+\frac{k_2d_k}{2}\right)\\
&\quad - (\mu+d+r)\left(a_{z+1}+\frac{n_2d_k}{2}\right) + (1-f)\phi\left(a_{z+1}+\frac{l_2d_k}{2}\right),\\
p_3 &= r\left(a_{z+1}+\frac{n_2d_k}{2}\right) - \mu\left(a_{z+1}+\frac{p_2d_k}{2}\right),\\
k_4 &= \Omega - \left(\frac{\alpha}{N}(a_{z+1}+n_3d_k)+\mu\right)(a_{z+1}+k_3d_k) + f\phi(a_{z+1}+l_3d_k),\\
l_4 &= \frac{\alpha}{N}(a_{z+1}+n_3d_k)q(1-p)(a_{z+1}+k_3d_k) - (\mu+\tau+\phi)(a_{z+1}+l_3d_k),\\
m_4 &= \frac{\alpha}{N}(a_{z+1}+n_3d_k)(1-q)(1-p)(a_{z+1}+k_3d_k) - (\mu+\gamma)(a_{z+1}+m_3d_k),\\
n_4 &= \tau(a_{z+1}+l_3d_k) + \gamma(a_{z+1}+m_3d_k) + \frac{\alpha}{N}(a_{z+1}+n_3d_k)p(a_{z+1}+k_3d_k)\\
&\quad - (\mu+d+r)(a_{z+1}+n_3d_k) + (1-f)\phi(a_{z+1}+l_3d_k),\\
p_4 &= r(a_{z+1}+n_3d_k) - \mu(a_{z+1}+p_3d_k).
\end{aligned}$$

Hence, the Eq. (17) is a numerical solution of the proposed mathematical model.

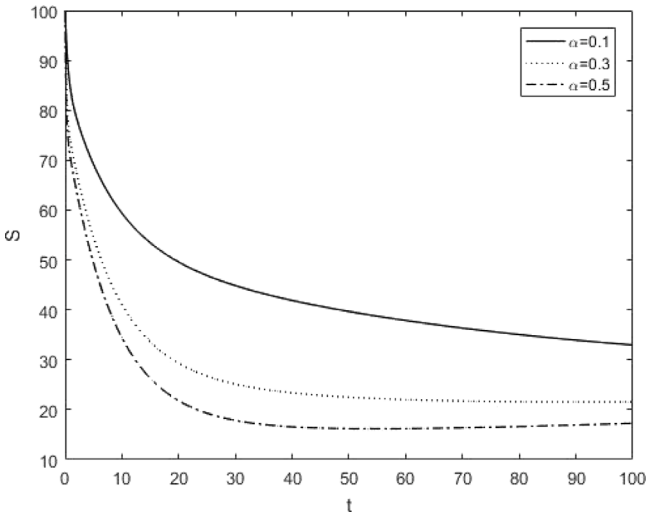

Fig. 1. Effect of α on S.

Figs. 1–16 demonstrate the simulations of different biological parameters on the different populations. Further, we will discuss the effect of these state variables on different biological parameters in the preceding figures.

In Figs. 1–3 we observe the effects of α, f and ϕ on S. Now, Fig. 1 explicit that as we increase the value of infection contact rate, the graph of susceptible class decreases. Fig. 2 demonstrates that vaccination has a significant effect on the susceptible population as the susceptible population increases as we increase the vaccination programme among the masses. Fig. 3 shows the variation of the susceptible population with respect to the death rate induced by COVID-19. It is clear that the COVID-19 cause mortality rate has demonstrated effects in susceptible cases.

Figs. 4–7 depict the effect of various populations on E_H classes. Fig. 4 indicates that the exposed population exponentially decrease up to $t = 10$ and it remains constant afterwards, as we increase the value of q. In Fig. 5 it is seen that E_H decays exponentially up to $t = 30$ and remains constant afterwards. Similarly, in Figs. 6 and 7, similar trends can be seen. In Figs. 6 and 7, we see the effects of α and ϕ on transmission dynamics of the COVID-19 class. Fig. 8 exhibits that the COVID-19 class curve decreases as we decrease the infection rate value from 0.1 to 0.001. Also, similar effects can be seen in Fig. 10

Figs. 10–14 show the effects of various parameters α, f, τ, γ and ϕ on I. In Fig. 10, we observe that as we rise the utility of progression rate from exposed tuberculosis class to infectious class rate, the graph

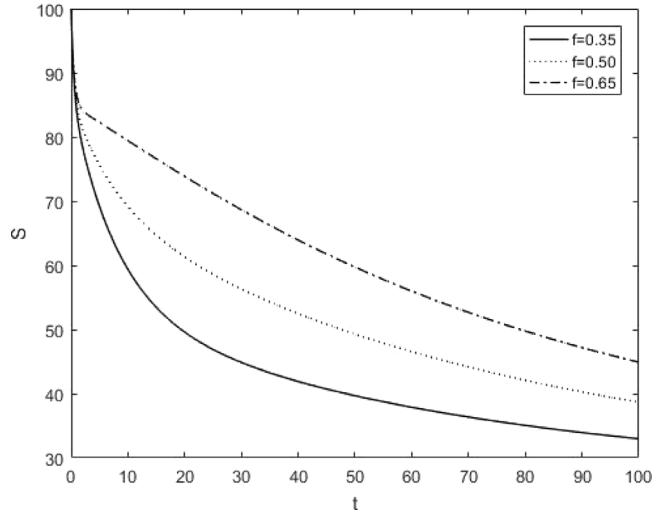

Fig. 2. Effect of f on S.

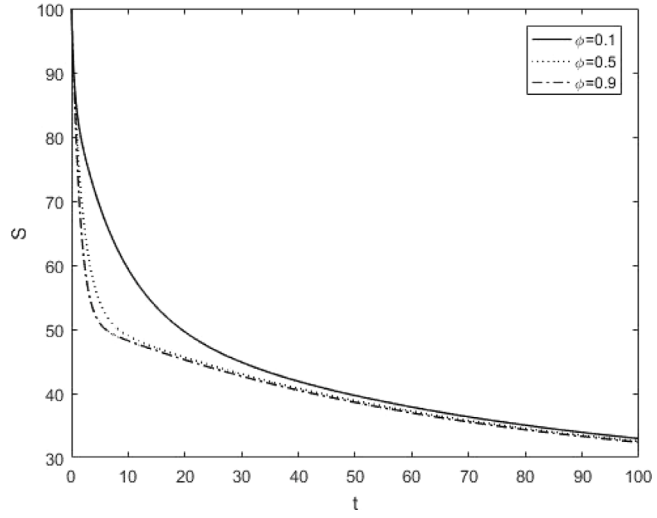

Fig. 3. Effect of ϕ on S.

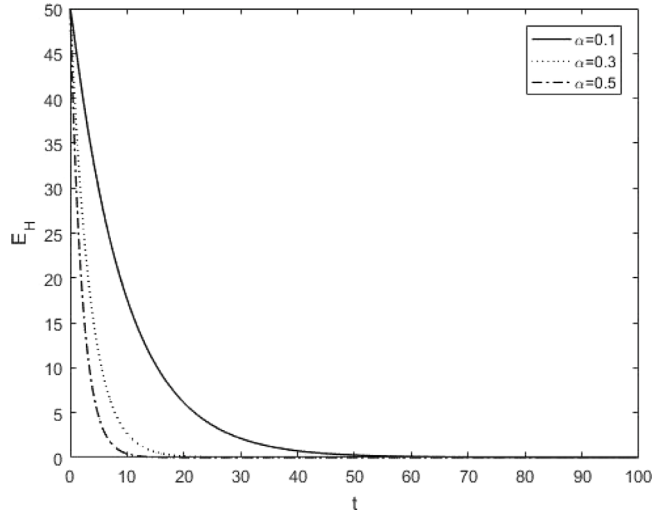

Fig. 4. Effect of α on S.

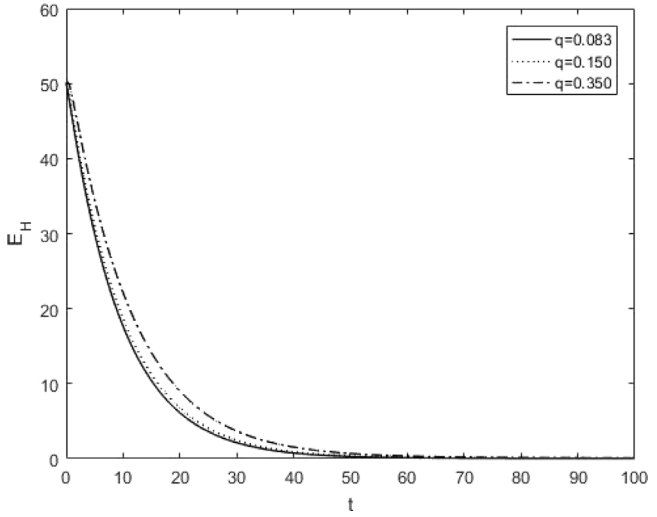

Fig. 5. Effect of q on E_H.

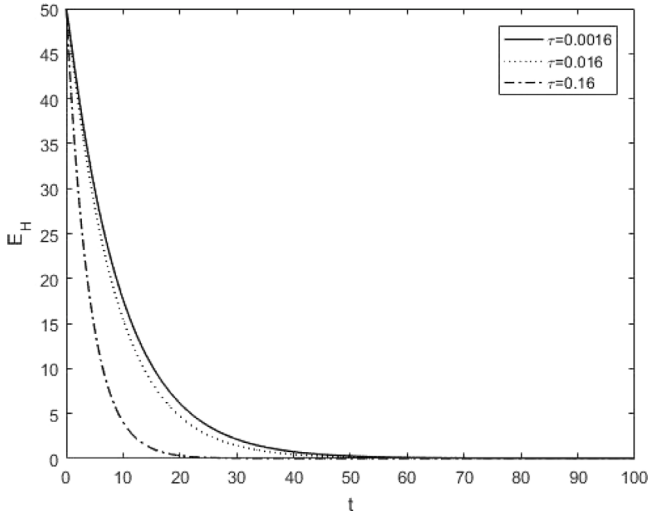

Fig. 6. Effect of τ on E_H.

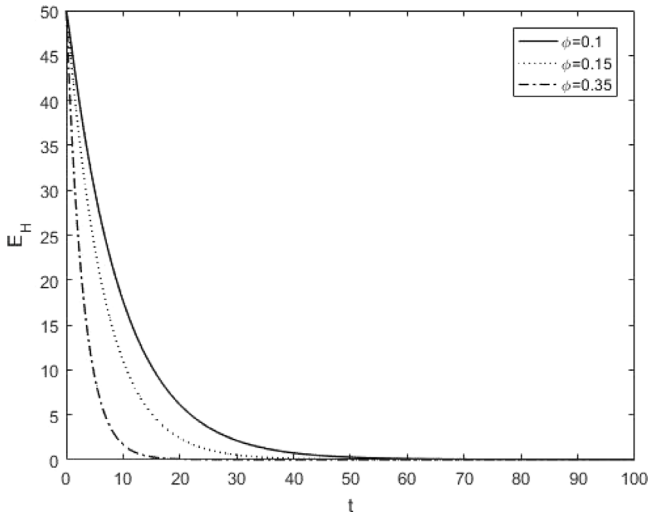

Fig. 7. Effect of ϕ on E_H.

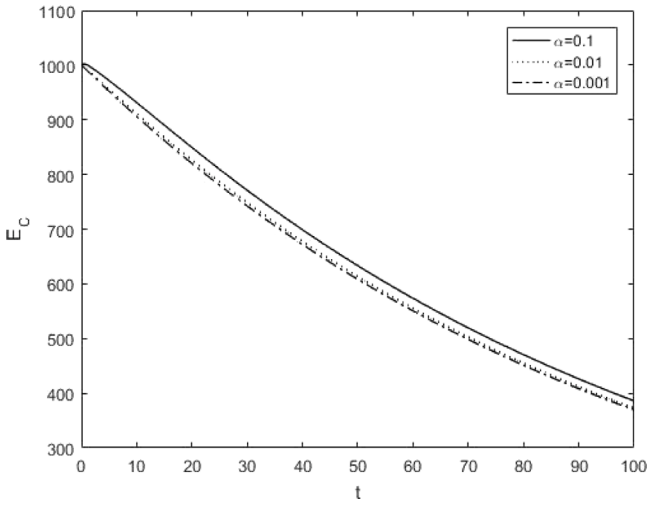

Fig. 8. Effect of α on S.

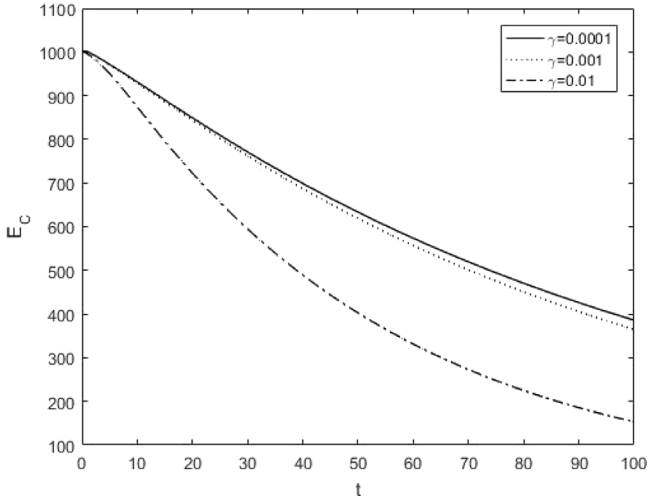

Fig. 9. Effect of γ on E_C.

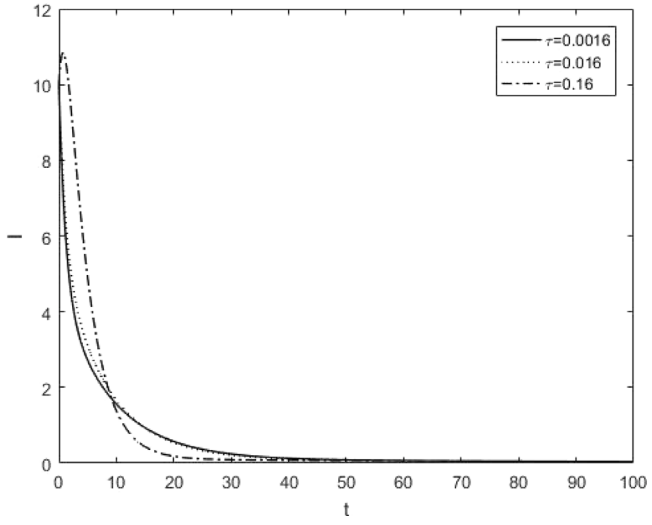

Fig. 10. Effect of α on S.

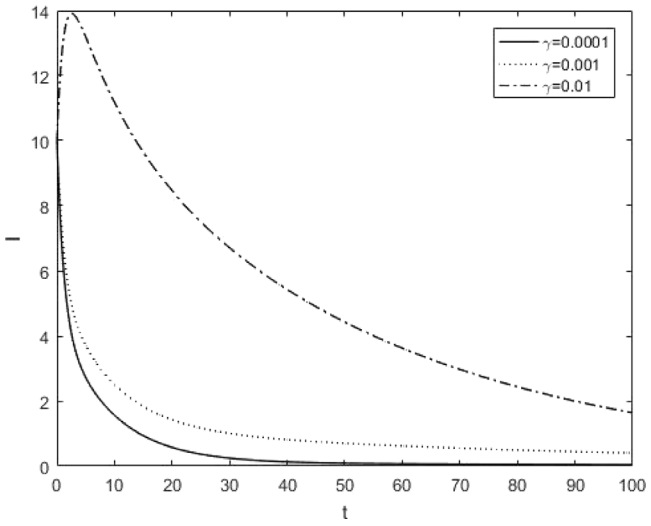

Fig. 11. Effect of f on S.

of infectious human class increases. In Fig. 11, we observe that as we rise the utility of progression rate from exposed COVID-19 population to infectious population, the graph of infectious human class increases. In Fig. 12, we observe that as we increase the value of infection contact rate, the graph of infectious human class decreases. In Fig. 13, we observe that as we increase the value of fast progress to the active disease rate, the graph of infectious human class decreases. From Fig. 14 we observe that as we rise the value of recovery rate from infectious class rate, the graph of infectious human class decreases.

In Fig. 15, we observe that as we rise the value of recovery rate from infectious class rate, the graph of recovered human class increases. Fig. 16 depicts that as we increase the value of COVID-19 causing mortality rate, the graph of recovered human class decreases.

In order to show the stability of disease-free critical point, we take $\alpha = 0.5, q = 0.083, (1-p) = 0.65, \mu = 0.00987, N = 2.739$ and $\Omega = 0.273$ by keeping other parameters fixed. We obtained the values of $\mathcal{R}_0 = 0.521$ and $E_0 = (27.659, 0, 0, 0, 0)$. From this, we can infer that E_0 is unstable. The stability of the positive critical point is E_1 and is computed as $(1.121, 49.684, 6808.8203, 30.653, 555.5)$.

9. Conclusion

In this paper, a novel SE_HE_CIR non-linear mathematical epidemic model for transmission dynamics of COVID-19 and tuberculosis is analysed. The essential basic control measures need to be highlighted particularly in tuberculosis cases. The tuberculosis hospitals and medication centres are required to be in early management and identification of COVID-19 in tuberculosis patients. It is also found that if we quarantine the TB-infected individual, they could be avoided the COVID-19 infection. In sensitivity analysis, we have seen that the rate of infection has significant effects on the propagation of COVID-19 transmission. We see that a small change in infective rate has a larger effect on COVID-19 transmission. It means that COVID-19 infection is spreading at a faster rate as compared to TB infection. Further, from our simulation, we computed the value of $\mathcal{R}_0 = 0.521$ which indicates that COVID-19 can be controlled through proper immunization and vaccination programmes. Our study further suggests that the need of the hour is to control SAR-CoV-2 viruses as it weakens the immunity which acts as a launching pad for other diseases. The use of optimal control helps us to find a better solution to deal with such a COVID-19 pandemic.

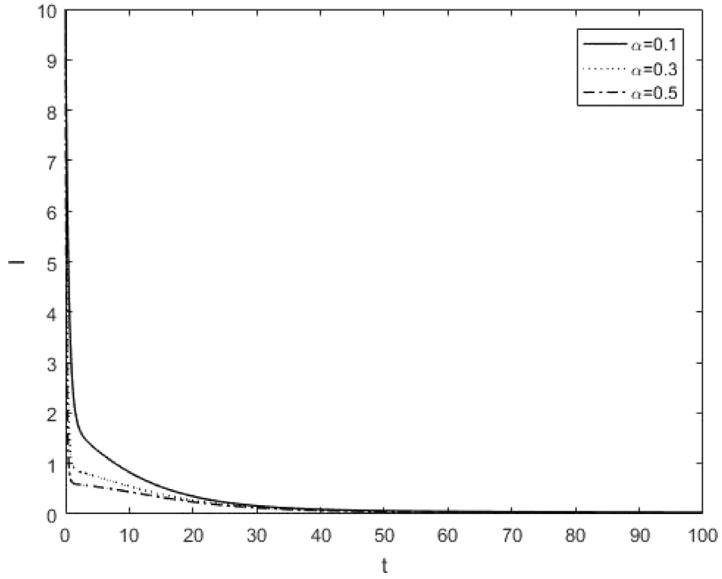

Fig. 12. Effect of α on S.

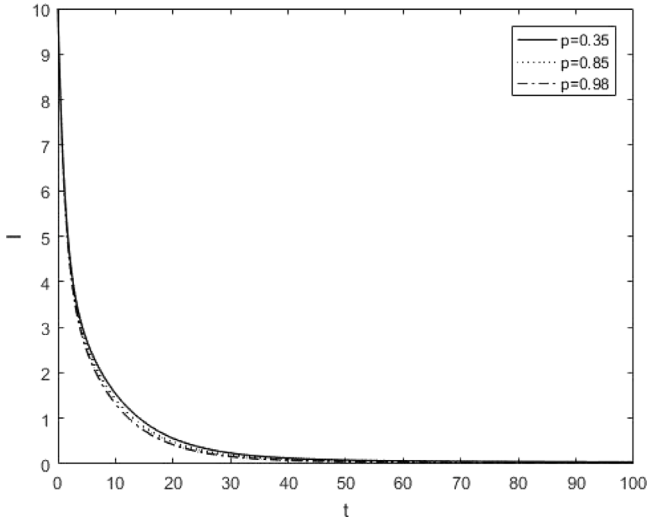

Fig. 13. Effect of p on I.

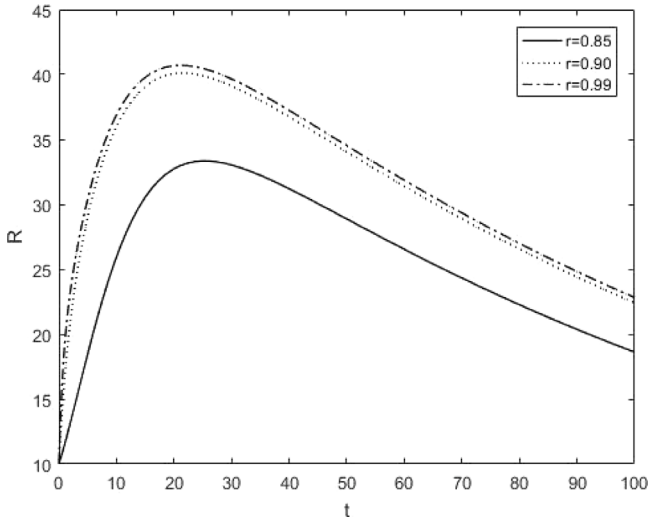

Fig. 15. Effect of r on I.

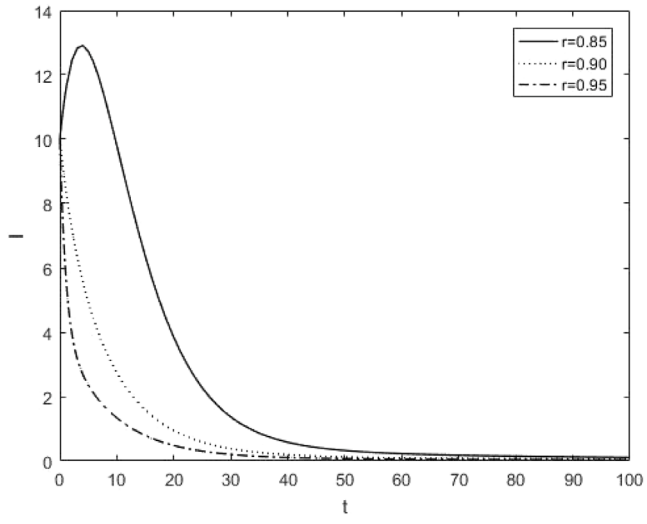

Fig. 14. Effect of r on I.

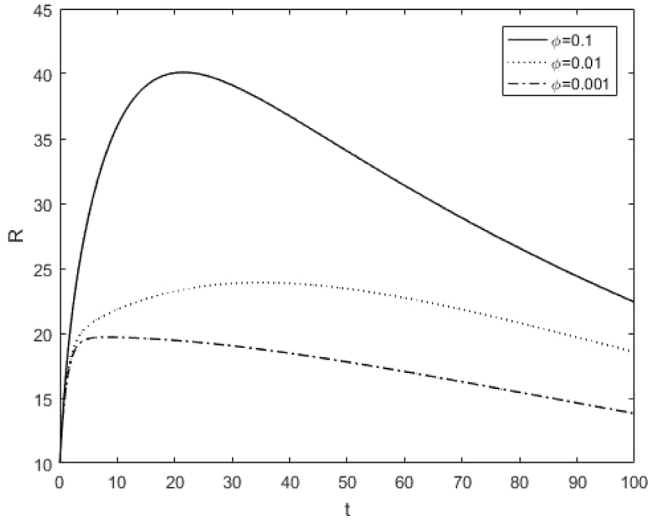

Fig. 16. Effect of ϕ on R.

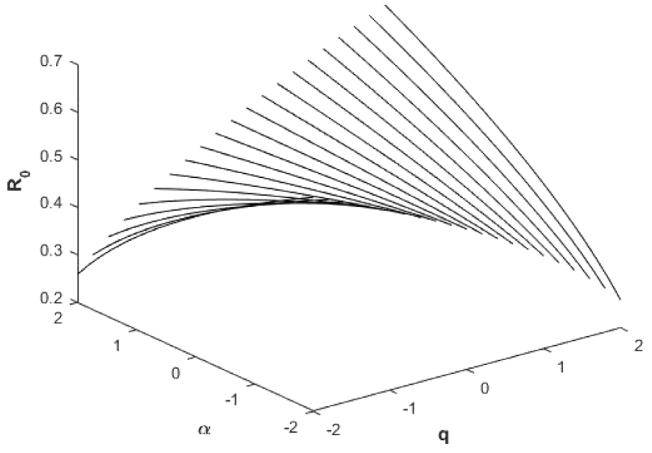

Fig. 17. Influence of q for α and $\mathcal{R}_0$.

Ethical approval

This article does not contain any studies with human participants or animals performed by any of the authors.

Informed consent

Informed consent was obtained from all individual participants included in the study.

Declaration of competing interest

The authors declare that they have no known competing financial interests or personal relationships that could have appeared to influence the work reported in this paper.

Data availability

Data is available from the authors upon reasonable request.

Appendix A

Consider the Lyapunov function

$$V_1 = \frac{1}{2}a_1V^2 + \frac{1}{2}a_2W^2 + \frac{1}{2}a_3X^2 + \frac{1}{2}a_4Y^2 + \frac{1}{2}a_5Z^2,$$

where, a_1, a_2, a_3, a_4, a_5, are arbitrary constants and V is the transformed susceptible individuals, W is the transformed exposed TB individuals, X is the transformed exposed Covid-19 individuals, Y is the transformed infected individuals, Z is the transformed recovered individuals. Therefore,

$$\begin{aligned}\dot{V}_1 =& a_1V\dot{V} + a_2W\dot{W} + a_3X\dot{X} + a_4Y\dot{Y} + a_5Z\dot{Z}\\ =& -\frac{1}{2}A_{11}V^2 + A_{12}VW + A_{14}VY - \frac{1}{2}A_{22}W^2 + A_{24}WY\\ &- \frac{1}{2}A_{33}X^2 + A_{34}XY + A_{42}WY + A_{43}XY - \frac{1}{2}A_{44}Y^2\\ &+ A_{54}ZY - \frac{1}{2}A_{55}Z^2,\end{aligned}$$

where, $A_{11} = 2a_1\mu$, $A_{12} = a_1f\phi$, $A_{14} = -a_1\frac{\alpha\Omega}{N\mu}$, $A_{22} = 2a_2(\mu+\tau+\phi)$, $A_{24} = a_2q(1-p)\frac{\alpha\Omega}{N\mu}$, $A_{33} = 2a_3(\mu+\gamma)$, $A_{34} = a_3\frac{\alpha\Omega}{N\mu}(1-q)(1-p)$, $A_{42} = a_4\big(\tau+(1-f)\big)$, $A_{43} = a_4\gamma$, $A_{44} = 2a_2(\mu+d+r)$, $A_{54} = a_5r$, $A_{55} = 2a_5\mu$.

The condition for $\dot{V}_1$ to be negative definite is that

$A_{12}^2 < A_{11}A_{22}$, $A_{14}^2 < A_{11}A_{44}$, $A_{24}^2 < A_{22}A_{44}$, $A_{34}^2 < A_{33}A_{44}$, $A_{42}^2 < A_{44}A_{22}$, $A_{43}^2 < A_{44}A_{33}$, $A_{54}^2 < A_{55}A_{44}$.

This gives the conditions for the trivial critical point $\bar{E}\left(\frac{\Omega}{\mu}, 0, 0, 0, 0\right)$ to be globally asymptotically stable.

Appendix B

Consider the Lyapunov function

$$V_2 = \frac{1}{2}b_1P^2 + \frac{1}{2}b_2Q^2 + \frac{1}{2}b_3R^2 + \frac{1}{2}b_4S^2 + \frac{1}{2}b_5T^2,$$

where, b_1, b_2, b_3, b_4, b_5 are arbitrary constants and V is the transformed susceptible individuals, W is the transformed exposed TB individuals, X is the transformed exposed Covid-19 individuals, Y is the transformed infected individuals, Z is the transformed recovered individuals. Therefore,

$$\begin{aligned}\dot{V}_2 =& b_1P\dot{P} + b_2Q\dot{Q} + b_3R\dot{R} + b_4S\dot{S} + b_5T\dot{T}\\ =& -\frac{1}{2}B_{11}P^2 + B_{12}PQ + B_{14}PS - \frac{1}{2}B_{22}Q^2 + B_{24}QS\\ &- \frac{1}{2}B_{33}R^2 + B_{34}RS + B_{42}QS + B_{43}RS - \frac{1}{2}B_{44}S^2\\ &+ B_{54}TS - \frac{1}{2}B_{55}T^2,\end{aligned}$$

where, $B_{11} = 2b_1\mu$, $B_{12} = b_1f\phi$, $B_{14} = -b_1\frac{\alpha\Omega}{N\mu}$, $B_{22} = 2b_2(\mu+\tau+\phi)$, $B_{24} = b_2q(1-p)\frac{\alpha\Omega}{N\mu}$, $B_{33} = 2b_3(\mu+\gamma)$, $B_{34} = b_3\frac{\alpha\Omega}{N\mu}(1-q)(1-p)$, $B_{42} = b_4\big(\tau+(1-f)\big)$, $B_{43} = b_4\gamma$, $B_{44} = 2b_2(\mu+d+r)$, $B_{54} = b_5r$, $B_{55} = 2b_5\mu$.

The condition for $\dot{V}_2$ to be negative definite is that

$B_{12}^2 < B_{11}B_{22}$, $B_{14}^2 < B_{11}B_{44}$, $B_{24}^2 < B_{22}B_{44}$, $B_{34}^2 < B_{33}B_{44}$, $B_{42}^2 < B_{44}B_{22}$, $B_{43}^2 < B_{44}B_{33}$, $B_{54}^2 < B_{55}B_{44}$.

Hence the conditions for the positive equilibrium E^* to be globally asymptotically stable.

References

[1] Adhikari SP, Meng S, Wu YJ. Epidemiology, causes, clinical manifestation and diagnosis, prevention and control of coronavirus disease (COVID-19) during the early outbreak period: a scoping review.. Infect Dis Pov 2020;17:1–12.
[2] World Health Organization. Coronavirus Disease 2019 (COVID19) Situation Report 92. Available from: https://www.who.int/docs/default-source/coronaviruses/situationreports/20200421-sitrep-92-COVID-19,2020.pdf?sfvrsn38e6b06d-4.
[3] Coronavirus Resource Centre. Available from: https://coronavirus.jhu.edu/map.html [Internet] [cited 2020 Apr 25, 2020].
[4] Liu Y, Bi L, Chen Y. Active or latent tuberculosis increases susceptibility to COVID-19 and disease severity. 2020, http://dx.doi.org/10.1101/2020.03.10.20033795, Med. Rxiv., 16.
[5] Guan W, Liang W, Zhao Y. Comorbidity and its impact on 1590 patients with COVID-19 in China: a nationwide analysis. Eur Respir J 2020;26:2000547.
[6] World Health Organization. Global Tuberculosis Report-2019. Available from: https://apps.who.int/iris/bitstream/handle/10665/329368/9789241565714-eng.pdf?ua1.
[7] Central TB Division. India TB Report 2019; 2019 Jun [Internet]. New Delhi [cited 2020 Apr 17]. Available from: https://tbcindia.gov.in/WriteReadData/India-TB-Report2019.pdf.
[8] Chadha VK. Tuberculosis epidemiology in India: a review. Int J Tuberc Lung Dis 2005;9:1072–82.
[9] Li Q, Guan X, Wu P. Early transmission dynamics in Wuhan, China, of novel coronavirus infected pneumonia. N Engl J Med 2020;29:1–9.
[10] Mandal S, Bhatnagar T, Arinaminpathy N, et al. Transmission in India: a mathematical model-based approach, prudent public health intervention strategies to control the coronavirus disease. Indian J Med Res 2019;151:190–9.
[11] Marimuthu Y, Nagappa B, Sharma N, et al. COVID-19 and tuberculosis: A mathematical model-based forecasting in Delhi, India. Indian J Tuberc 2020;67:177–81.
[12] Rehman AU, Singh R, Abdeljawad T, et al. Modeling, analysis and numerical solution to malaria fractional model with temporary immunity and relapse. Adv Diff Equ 2021;2021:390.
[13] Walaza S, Cohen C, Tempia S. Influenza and tuberculosis co-infection: a systematic review influenza other respi. Viruses 2020;14:77–91.
[14] Arkapal B, Sarika P, Krishna B, Shailendra H. COVID-19 and tuberculosis co-infection: a neglected paradigm. Monaldi Arch Chest Dis 2020;90:518–22.
[15] Liu Y, Yan LM, Wan L. Viral dynamics in mild and severe cases of COVID-19. Lancet Infect Dis 2020;19:656–7.
[16] Chopra KK, Arora VK, Singh S. COVID 19 and tuberculosis. Indian J Tuberc 2020;67:149–51.
[17] Acheampong E, Okyere E, Iddi S, et al. Mathematical modelling of earlier stages of COVID-19 transmission dynamics in Ghana. Results in Phys 2022;34:105193.
[18] Faniran TS, Ali A, Al-Hazmi NE, et al. New variant of SARS-CoV-2 dynamics with imperfect vaccine complexity, 1062180. 2022.

[19] Moore SE, Nyandjo-Bamen HL, et al. Global stability dynamics and sensitivity assessment of COVID-19 with timely-delayed diagnosis in ghana computational and mathematical biophysics. Results in Phys 2022;10:87–104.
[20] WHO. World Health Organization (WHO) Information Note Tuberculosis and COVID-19: Considerations for Tuberculosis (TB) Care. Available from https://www.who.int/tb/COVID-19considerationstuberculosisservices.pdf.
[21] Hellewell J, Abbott S, Gimma A. Feasibility of controlling COVID-19 outbreaks by isolation of cases and contacts. Lancet Glob Health 2020;1:8(4):e488ee496.
[22] Rehman AU, Singh R, Singh J. Mathematical analysis of multi-compartmental malaria transmission with reinfection. Chaos Solitons Fractals 2022;163(2):112527.
[23] Sharma N, Pathak R, Singh R. Modeling of media impact with stability analysis and optimal solution of SEIRS epidemic model. J Interdiscip Math 2019;22:1123–56.
[24] Singh R, Sharma N, Gosh A. Mathematical analysis and mitigation through intervention: An application to ebola type infectious disease. Lett Biomath 2019;6:1–19.
[25] Agarwal P, Singh R. Modeling of transmission dynamics of nipah virus(Niv): A fractional-order approach. Physica A 2020;547:124243.
[26] Agarwal P, Singh R, Rehman AU. Numerical solution of a hybrid mathematical model of dengue transmission with relapse and memory via Adam–Bashforth–Moulton predictor–corrector. Chaos Solitons Fractals 2021;143:110564.
[27] Mwenyeheri T, Shaban N, Hove-Msekwa D, et al. Formulation of mathematical model for TB transmission in zoonotic areas with existence of endemic equilibrium. J Tuberc Res 2014;2:132–43.
[28] Driessche PV, Watmough J. Reproduction numbers and sub-threshold endemic equilibria for compartmental models of disease transmission. Math Biosci 2002;180:29–48.
[29] John WC, Peter N, Banda K. Eararky deaths during tuberculosis treatment are associated with depressed innate responses, bacterial infection, and tuberculosis progression. J Infect Dis 2011;1:204(3):358e362.
[30] Yang X, Yu Y, Xu J. Clinical course and outcomes of critically ill patients with SARS-CoV-2 pneumonia in Wuhan, China: a single-centered, retrospective, observational study. Lancet Resp Med 2020;8:475–81.
[31] Ndairou F, Area I, Nieto J, Torres DFM. Mathematical modeling of COVID-19 transmission dynamics with a case study of Wuhan. Chaos Solitons Fractals 2020;135:109846.
[32] Rehman AU, Singh R, Agarwal P. Modeling, analysis and prediction of new variants of COVID-19 and dengue co-infection on complex network. Chaos Solitons Fractals 2021;150:111008.
[33] Asamoah JKK, Owusu MA, Jin Z, et al. Global stability and cost-effectiveness analysis of COVID-19 considering the impact of the environment: using data from Ghana. Chaos Solitons Fractals 2020;140:110103.
[34] Asamoah JKK, Jin Z, Sun G-Q, et al. Sensitivity assessment and optimal economic evaluation of an new COVID-19 compartmental epidemic model with control interventions. Chaos Solitons Fractals 2021;146:110885.
[35] Asamoah JKK, Okyere E, Abidemi A, et al. Optimal control and comprehensive cost-effectiveness analysis for COVID-19. Results Phys 2022;33(1):105177.
[36] Asamoah JKK, Bornaa CS, Seidu B, et al. Mathematical analysis of the effects of controls on transmission dynamics of SARS-CoV-2. Alexandra Eng J 2020. http://dx.doi.org/10.1016/j.aej.2020.09.033.
[37] Asamoah JKK, Jin Z, G.-Q Sun. Non-seasonal and seasonal relapse model for Q fever disease with comprehensive cost-effective analysis. Results in Phys 2021;22:103889.
[38] Rocklov J, Sjodian H, Wilder-Smith A. COVID-19 outbreak on the diamond princess cruiseship: estimating the epidemic potential and effectiveness of public health counter measures. J Trav Med 2020;28:aaa030. http://dx.doi.org/10.1093/jtm/taaa030/5766334.